Converging Beam LIDAR for Increasing Offshore Wind Farm Yield and for Improving Safety and Utilisation in Offshore Crane Operation

Dr Theodore Holtom[1,2], Dr Henry Bookey[3], Dr Anthony Brooms[4], Benn Faulkner[5]
[1]Wind Farm Analytics Ltd, [2]Triple LIDAR Technology Ltd, [3]Fraunhofer UK Research Ltd, [4]Birkbeck, University of London, [5]Renewable Advice Ltd

Abstract

This poster updates the offshore wind industry on progress to date in developing converging beam Doppler LIDAR 3d wind measurement technology, its theoretical basis and why this is a significant improvement over existing diverging beam LIDARs. A value proposition will be explained to show how offshore wind farm energy yield may be increased by around 10%. R&D progress will be outlined including cable robot testing simulating 5 metre wave motion. Furthermore the team is also researching the application of this technology to achieve simultaneously safer and more efficient crane operations, which are presently operationally limited by basic wind measurement.

Objectives

Specialists and practitioners in the field of LIDAR wind measurement have appreciated that the existing LIDAR systems used within the wind industry suffer from "implicit wind field homogeneity assumption" [1, Wagenaar et al] – conical scans and VAD beam swinging designs all combine multiple line of sight wind velocity components from around a large sampling circle which would be fine if and only if the wind velocity field were constant around that circle. In reality the wind velocity varies substantially as can be appreciated by observing the wind across a tree, witnessing the varying wind direction and intensity from top to bottom and from left to right across the branches of the tree. Meanwhile large structures such as wind turbine rotors, and indeed construction cranes, are much larger than a tree so the variability of the wind field across such structures is important.

The converging beam approach, where all three velocity components are collected from three separate Doppler LIDARs aimed at a given measurement point, allows correct three-dimensional wind velocity reconstruction without ambiguities or assumptions of uniform wind field. By collecting converging beam wind velocity measurements from multiple points in space one can build a map of the three-dimensional wind velocity field and understand better the variation of the wind in space. Important attributes of the wind such as turbulence and wind shear may be much better directly measured using the converging beam approach [2, Sathe et al].

There are multiple objectives relevant to improving offshore wind projects:

- Eliminating serious ambiguities existing in current LIDAR measurements, increasing accuracy and reducing P50 energy yield uncertainty.
- Also reducing investor risk by checking wind conditions are appropriate up to top tip height including gusts, turbulence, wind shear, etc.
- Improving annual energy yield by accounting for wind direction variability across the entire rotor.
- Reducing lifetime fatigue loading by look ahead alarms of the most damaging inflow allowing protective control, increasing asset lifetime
- Reducing O&M costs, enabling cheaper turbines, more accurate storm shutdown / re-start
- Improving crane safety, improving crane efficiency.

For each Doppler unit vector $\hat{\mathbf{r}}_i$, $i \in \mathcal{I}$, we may characterize its direction by: $\theta_i \in [0, 2\pi)$, the azimuthal angle measured anti-clockwise from the x-axis; $\phi_i \in [-\pi/2, \pi/2]$, the elevation angle from the (x,y)-plane, taken to be positive when the z-coordinate is positive (as would normally be the case for a platform set on the ground measuring a point that is above ground). Then each of the Doppler unit vectors can be re-expressed in terms of the standard basis as follows:

$$\hat{\mathbf{r}}_i = \cos(\theta_i)\cos(\phi_i)\mathbf{e}_1 + \sin(\theta_i)\cos(\phi_i)\mathbf{e}_2 + \sin(\phi_i)\mathbf{e}_3 \quad i \in \mathcal{I}. \tag{3}$$

Equations (2) and (3) can also be written in matrix form:

$$\widetilde{\mathbf{v}} = \mathbf{M}\mathbf{v} \tag{4}$$

where

$$\mathbf{M}_{i1} = r_{i1} = \cos(\theta_i)\cos(\phi_i), \quad i \in \mathcal{I} \tag{5}$$

$$\mathbf{M}_{i2} = r_{i2} = \sin(\theta_i)\cos(\phi_i), \quad i \in \mathcal{I} \tag{6}$$

$$\mathbf{M}_{i3} = r_{i3} = \sin(\phi_i), \quad i \in \mathcal{I} \tag{7}$$

and

$$\widetilde{v}_i = \sum_{j\in\mathcal{I}} \mathbf{M}_{ij} v_j = \cos(\theta_i)\cos(\phi_i)v_1 + \sin(\theta_i)\cos(\phi_i)v_2 + \sin(\phi_i)v_3, \quad i \in \mathcal{I}. \tag{8}$$

It will be assumed throughout the remainder of this paper that $\mathbf{M}$ *is of full rank.*

Thus, given the 6 Doppler angles and the 3 Doppler wind velocity coordinates, one can determine the equivalent co-ordinate representation of the wind velocity with respect to the standard basis:

$$\mathbf{v} = \mathbf{M}^{-1}\widetilde{\mathbf{v}} \tag{9}$$

or, equivalently,

$$v_j = \sum_{k\in\mathcal{I}} [\mathbf{M}^{-1}]_{jk}\widetilde{v}_k \quad j \in \mathcal{I}. \tag{10}$$

Figure 5 – 3d velocity reconstruction requires 3 lines of sight

Figure 6 – crane operations need good wind measurement

where

$$s^2_{v_j}(\boldsymbol{\theta}_0, \boldsymbol{\phi}_0, \widetilde{\mathbf{v}}_0) = \sum_{n\in\mathcal{I}} \left\{ \left(\frac{\partial v_j}{\partial \theta_n}\right)^2 \sigma^2_{\theta_n} + \left(\frac{\partial v_j}{\partial \phi_n}\right)^2 \sigma^2_{\phi_n} + \left(\frac{\partial v_j}{\partial \widetilde{v}_n}\right)^2 \sigma^2_{\widetilde{v}_n} \right\}\Bigg|_{(\boldsymbol{\theta}_0, \boldsymbol{\phi}_0, \widetilde{\mathbf{v}}_0)}. \tag{17}$$

The expression for $s^2_{v_j}(\boldsymbol{\theta}_0, \boldsymbol{\phi}_0, \widetilde{\mathbf{v}}_0)$ corresponds to the standard expression for the *error propagation formula* (c.f. Taylor (1997)): typically, formulae such as these are derived by truncating the expression for $v_j(\boldsymbol{\theta}^*, \boldsymbol{\phi}^*, \widetilde{\mathbf{v}}^*)$ at first order and finding the variance of just that, without actually taking higher order terms into account, unlike our account of the result. **The calculation of $s^2_{v_j}(\boldsymbol{\theta}_0, \boldsymbol{\phi}_0, \widetilde{\mathbf{v}}_0)$ will be the focus of our discussion for the remainder of this paper.**

Along with the values of the variances of the six angles and those of the three measured Doppler velocity components, it is also required to evaluate the partial derivatives that appear in (17).

$$\frac{\partial v_j}{\partial \theta_s} = \sum_{k\in\mathcal{I}} \frac{\partial\{[\mathbf{M}^{-1}]_{jk}\widetilde{v}_k\}}{\partial \theta_s} = \sum_{k\in\mathcal{I}} \widetilde{v}_k \frac{\partial [\mathbf{M}^{-1}]_{jk}}{\partial \theta_s} + \sum_{k\in\mathcal{I}} [\mathbf{M}^{-1}]_{jk} \frac{\partial \widetilde{v}_k}{\partial \theta_s} \tag{18}$$

$$\frac{\partial v_j}{\partial \phi_s} = \sum_{k\in\mathcal{I}} \frac{\partial\{[\mathbf{M}^{-1}]_{jk}\widetilde{v}_k\}}{\partial \phi_s} = \sum_{k\in\mathcal{I}} \widetilde{v}_k \frac{\partial [\mathbf{M}^{-1}]_{jk}}{\partial \phi_s} + \sum_{k\in\mathcal{I}} [\mathbf{M}^{-1}]_{jk} \frac{\partial \widetilde{v}_k}{\partial \phi_s} \tag{19}$$

$$\frac{\partial v_j}{\partial \widetilde{v}_s} = \sum_{k\in\mathcal{I}} [\mathbf{M}^{-1}]_{jk} \frac{\partial \widetilde{v}_k}{\partial \widetilde{v}_s} = \sum_{k\in\mathcal{I}} [\mathbf{M}^{-1}]_{jk}\delta_{sk} \tag{20}$$

Figure 7 – minimise uncertainty in measurement campaigns

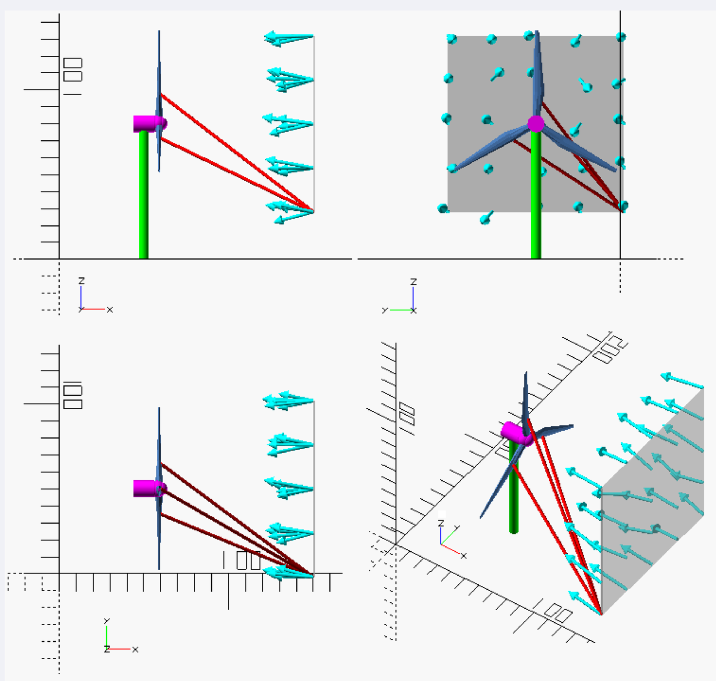

Figure 1 –forward looking 3d wind mapping/ scanning

Figure 2 – blade integration

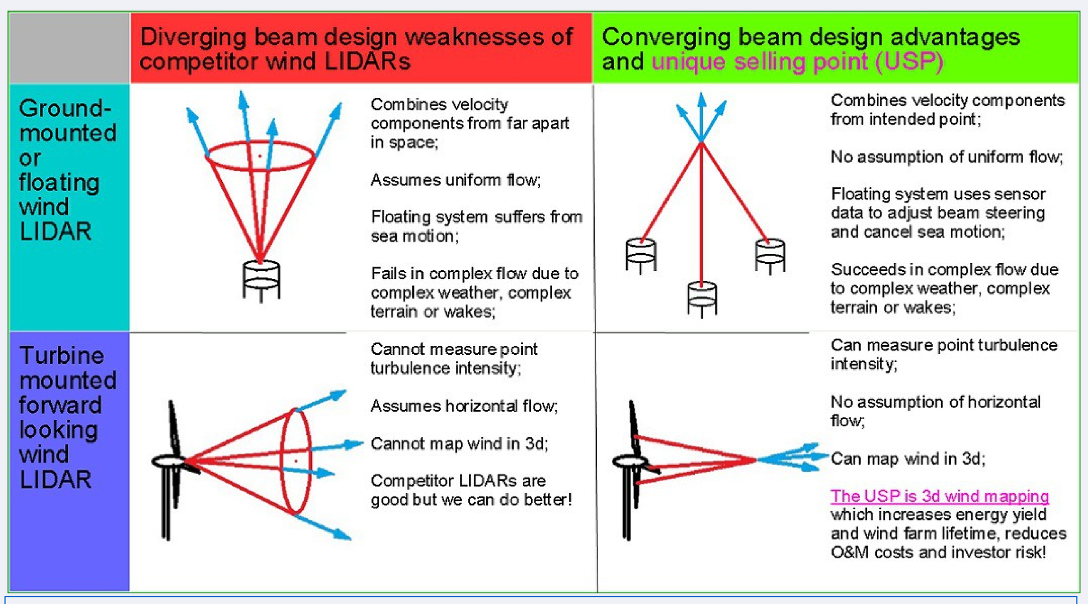

Figure 3 – weaknesses of diverging beam LIDAR (left) and strengths of converging beam LIDAR (right) both for ground/floating systems (above) and turbine mounted forward looking systems (below)

Figure 4 – cable robot sea state testing

Methods

A new converging beam Doppler LIDAR laser beam wind measurement has been conceptualised, designed, built and tested. The LIDAR beam steering component has also been built and tested. Computer simulations calculated typical floating platform / buoy motion in different sea states including high sea states as witnessed in the North Sea and typical offshore wind farm locations around the world. Large scale cable robots were used to test the system with 5m vertical motion combined also with angular motion typical of high sea states. As well as testing the beam steering LIDAR against a calibrated met mast on a Scottish wind farm work with blade experts confirms the system may be safely retrofitted or factory-integrated into the blades.

The team has highlighted to industry the mathematical basis and equations for wind measurement using converging beam LIDAR [3, Holtom & Brooms, 2019] – see Figures 5 and 7. The unique selling point of 3d wind mapping and advantages are shown in Figure 3, both at planning stage to reduce investor risk by better assessment of true wind conditions and at the operational stage when more advanced control can increase annual energy yield from the turbines whilst simultaneously reducing the fatigue loading so that the asset lives longer.

Conclusions

A strong customer value proposition exists for offshore wind farm investors. Firstly, at the planning stage better measurements of the site wind conditions allow to make sure they are suitable for the chosen wind turbines with regard to top tip height wind speeds, gusts and turbulence intensity measured without diverging beam LIDAR ambiguity and using sensors and beam steering to correct for floating platform sea motion. Secondly during operation the scanning converging beam LIDAR allows look ahead 3d mapping of the wind, thereby allowing increasing annual revenue by improved yaw control according to the full rotor wind direction. Thirdly look ahead alarms can be employed by the turbine control system in order to alleviate fatigue loading throughout the asset lifetime, thereby extending the asset lifetime and reducing O&M costs. Fatigue loading of wind turbines is roughly proportional to turbulence intensity, but also increases with wind shear, gusts and other wind attributes as well as their combinations. On this basis, informed by both operational data analysis as well as computer simulation of loads throughout the structure, it is estimated that energy yield can be increased by 10%. This can be worth £6 million per large offshore turbine whereas the system cost can be £100k.

The same technology can be applied in other industries too, such as helicopter operations and aviation runways. The team is presently studying how to improve safety and simultaneously how to increase utilisation of cranes during construction since crane operations are limited by wind. Because of much more advanced look ahead 3d laser wind mapping it will be possible to identify gusts and other threats to crane operational safety with greater certainty. By measuring the wind field more comprehensively and with greater certainty the safe operating limit for crane operations can be increased without compromising safety. It is envisaged that a follow on project may make direct load measurements on an operational crane to prove this claim.

The team invites collaboration from wind turbine owners, offshore wind farm developers and investors interested to undertake turbine demonstration of the rotor-integrated forward looking device and to undertake at-sea demonstration of the floating device in order to directly quantify the benefits and provide a customer case study. The team also invites collaboration from crane manufacturers and offshore installation crane operators and related stakeholders interested to witness proof of the claimed benefits via a project of direct measurement. Investors are also welcome in order to commercialise multiple patents for UK economic benefit and clean growth #MadeInGlasgow. Thanks to InnovateUK for funding towards progress to date.

References

1. Wagenaar et al, "Wind Iris nacelle LiDAR calibration at ECN test site", https://publications.ecn.nl/WIN/0/ECN-E--16-053 , 2016
2. Sathe et al, "Estimating Turbulence Statistics and Parameters from Ground- and Nacelle-Based Lidar Measurements: IEA Technical report, Technical University of Denmark, 2015
3. Holtom & Brooms, "Error Propagation Analysis for a Static Convergent Beam Triple LIDAR", Birkbeck Math. Sciences Preprint 41, http://eprints.bbk.ac.uk/25809/1/preprint41, 2019

renewableUK 2019 GLOBAL OFFSHORE WIND 25 – 26 June ExCeL London

Poster Competition – Global Offshore Wind 2019